THE OPTIMIZATION OF PRESSURE CONTROLLER FOR DEEP EARTH DRILLING

by

Zhi Qiang HE[a,b], Ling CHEN[c*], Tong LU[a,b], and Jing XIE[a,b]

[a] State Key Laboratory of Hydraulics and Mountain River Engineering, College of Water Resource and Hydropower, Sichuan University, Chengdu, China
[b] Key Laboratory of Deep Underground Science and Engineering (Sichuan University), Ministry of Education, Chengdu, China
[c] School of Mechanical Engineering, Sichuan University, China

Original scientific paper
https://doi.org/10.2298/TSCI180612123H

Obtaining samples of deep in-situ conditions is first step to explore the mysteries of the earth requires. In view of the current problems of insufficient pressure maintaining capacity of the existing equipment, we independently developed the in-situ fidelity coring system and designed the osmotic pressure controller based on the geometry of square cover. The finite element method is used to analyze the pressure maintaining capacity of the pressure controller. It is found that it would produce large deformation and stress concentration when the pressure was applied on, resulting in low pressure maintaining capacity. Then the structural optimization schemes of conical sealing contact surfaces with 25°, 35°, 40°, and 45° apex angles and spherical sealing contact surface are proposed, and the spherical contact surface structure is found to be optimal. Finally, the material is optimized, and a higher strength material such as 45CrNiMoVA alloy is used. Based on the pressure controller with spherical contact surface, the pressure maintaining capacity increased to nearly 70 MPa. The research results obtained in this paper provide the basis for the development of the coring system, the deep exploration of the earth and the establishment of rock mechanics theory.

Key words: *deep in-situ fidelity coring system, osmotic pressure controller, numerical simulation, optimization analysis*

Introduction

The shallow mineral resources of the earth has been gradually exhausted, and more and more attentions have been paid to the mineral exploitation in deep earth [1]. Deep mining is an on-going mining industry [2, 3]. At present, the basic research of deep mining is not sufficient, and it is necessary to establish a deep in-situ rock mechanics theoretical system. For example, the relationship between the mechanical environment and the fracture evolution of deep engineering rock mass is still unclear [4]. Therefore, it is essential to develop deep in-situ fidelity coring (maintaining in-situ osmotic pressure, *etc*.) system to maintaining in-situ conditions, which provides a basis for further test.

Scientific drilling has become an indispensable and important means for human beings to solve major problems such as resources, disasters and the environment. Drilling programs have caused widespread concern worldwide, Including Mohole Drilling Project,

* Corresponding author, e-mail: chenlingscu@scu.edu.cn

Deep Sea Drilling Project, and so on [5-9]. However, the strong mechanical disturbance of the traditional coring system destroys the authenticity of osmotic pressure [10]. In the field of deep drilling in the mainland, the main focus is still on the core drilling technology [11]. Only ocean drilling has taken the lead in focusing on seafloor sediment fidelity coring technology [12]. However, the pressure maintaining capacity of coring system has not been developed. hydrate auto-clave coring equipment (HY-ACE) used a fu-gro pressure corer (FPC) and rotary corer (HRC) with capacity of 25 MPa [13]. Japan developed the pressure temperature core sampler (PTCS) which has capacity of 30 MPa [14]. The capacity of the multiple autoclave corer (MAC) and the dynamic autoclave piston corer (DAPC) used by R.V.SONNE is 20 MPa [15, 16]. The pressure maintaining capacity of the fidelity corer designed, respectively, by Zhejiang University and The First Institute of Oceanography is 30 MPa [17-19].

It can be seen that the pressure maintaining capacity of the aforementioned coring system is not suitable to be applied for deep drilling in the mainland. Therefore, we independently developed the fidelity coring system and designed the osmotic pressure controller based on the geometry of square cover. The finite element method was used to analyze the pressure maintaining capacity of the pressure controller. Several optimization schemes were proposed for comparison, and the resulting optimization scheme with spherical contact surface structure was found to be optimal. The results obtained in this paper provide the basis for the development of the coring system, the deep exploration of the earth and the establishment of rock mechanics theory.

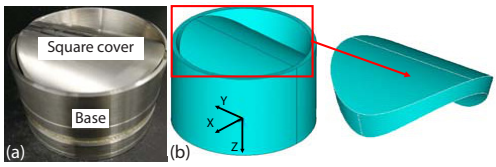

Figure 1. Pressure controller and numerical model; (a) pressure controller, (b) numerical model

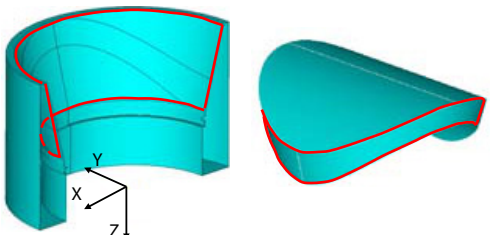

Figure 2. Sealing contact surface

Pressure maintaining capacity analysis of developed pressure controller

Model construction

Based on developed pressure controller, numerical model on ANSYS platform was built after appropriate simplification, as shown in fig. 1. Pressure controller consists of base and square cover. Height of base is 0.048 m. The inside and outside diameter is 0.0575 m and 0.0797 m. Inner sealing contact surface is a conical surface with a apex angle of 30° and bottom circle with diameter of 0.0745 m, and coincides with the upper surface of the base, as shown in fig. 2. There is a square cover structure placed above the pressure controller with thickness of 0.008 m. The bottom surface of the model is on the XOY plane, and the axis direction is in the negative direction of the *Z*-axis.

Calculation parameters and boundary conditions

As the main functional structure, pressure controller which has high load-bearing capacity must be suitable for the deep in-situ fidelity coring. The 20CrMnMo cementation steel was taken for pressure controller. Material parameters are shown in tab. 1. The bilinear kinematic hardening constitutive model was used to calculate the model.

Table 1. Material parameters

Materials	Elasticity modulus [Pa]	Poisson ratio	Density [kgm^{-3}]	Yield stress [Pa]	Shear modulus [Pa]
20CrMnMo	2.07e11	0.254	7.87e3	8.85e8	8.25e10

The hydrostatic pressures corresponding to the depths of 1000 m, 3000 m, 5000 m, 7000 m, and 10000 m are 10 MPa, 30 MPa, 50 MPa, 70 MPa, and 100 MPa. These pressures were separately applied on the upper surface of square cover and some part of the base surface according to actual situation. Contact was set between square cover and the base, as shown in fig. 2. Coefficient of friction is 0.12. Full displacement constraint was applied on the bottom of the base. The X, Y displacement constraint were applied to the side, as shown in fig. 3.

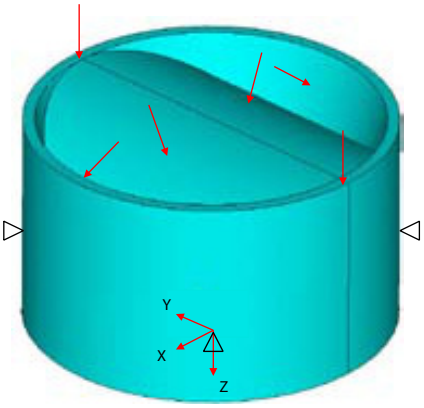

Figure 3. Schematic diagram of boundary conditions

Results

The axial displacement and von mises stress contours of square cover calculated under various pressure conditions are shown in fig. 4. Due to the limited space, the results at 10 MPa, 50 MPa, and 70 MPa are listed here.

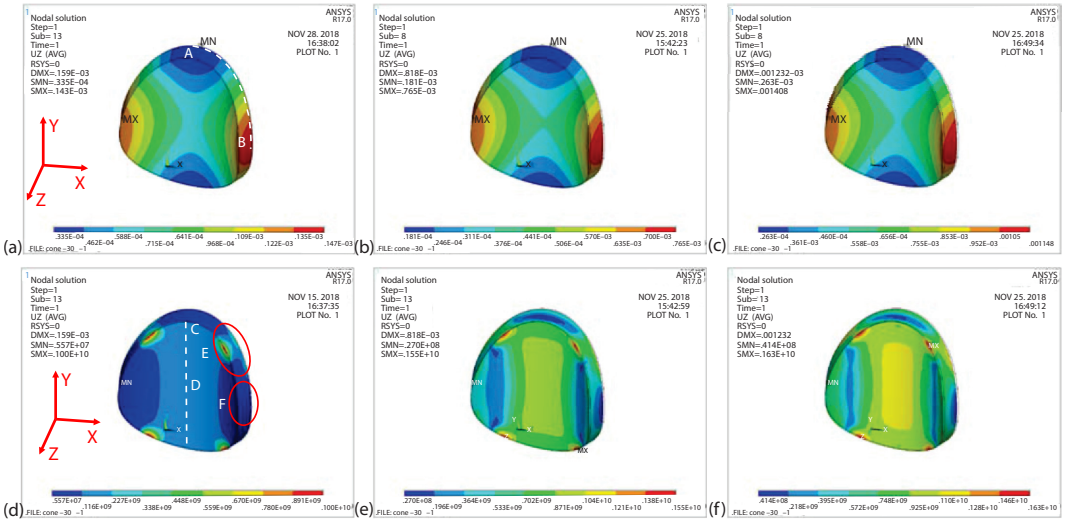

Figure 4. Axial displacement and Von Mises stress contours of square cover; (a) axial displacement contours (10 MPa), (b) axial displacement contours (50 MPa), (c) axial displacement contours (70 MPa), (d) Von Mises stress contours (10 MPa), (e) Von Mises stress contours (50 MPa), and (f) Von Mises stress, contours (70 MPa) (*for color image see journal web site*)

Square cover is a symmetrical structure. To study the position where the maximum deformation occurs, the node on the upper surface of the square cover was taken as the displacement monitoring point, shown by the dotted line (AB) in fig. 4(a). The results of nodal axial displacement under various conditions are shown in tab. 2 and fig. 5.

Table 2. Axial displacement of node on the square cover

Contents	Axial displacement of nodes [mm]				
	10 MPa	30 MPa	50 MPa	70 MPa	100 MPa
Minimum value	0.03	0.11	0.18	0.26	0.43
Maximum value	0.15	0.45	0.76	1.15	2.01
Difference	0.12	0.34	0.58	0.89	1.58

Illustrated by displacement contours in fig. 4, the maximum displacement value appears at the B point of upper surface of the square cover, while the displacement of the A point area is the smallest. As shown in tab. 2 and fig. 5, with the increase of pressure, the increasing trend of nodal displacement is more obvious and nodal displacement increases as well. The displacement differences between the maximum displacement and the minimum displacement of the node also significantly increase, which are 0.12 mm, 0.34 mm, 0.58 mm, 0.89 mm, and 1.58 mm, respectively. Axial displacement, *Z*-axis positive direction, appears at the square cover at the same time of deforming. Characteristics of base and square cover under pressure made a better fit of these two, keeping the in-situ pressure in stable.

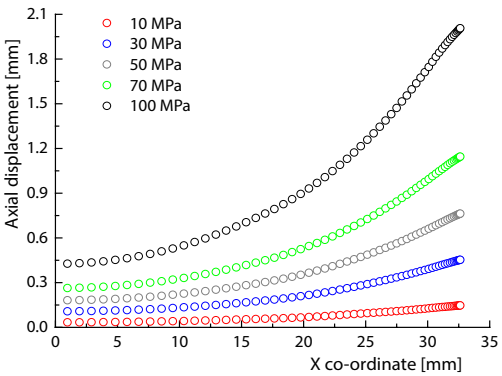

Figure 5. Axial displacement of node on the square cover

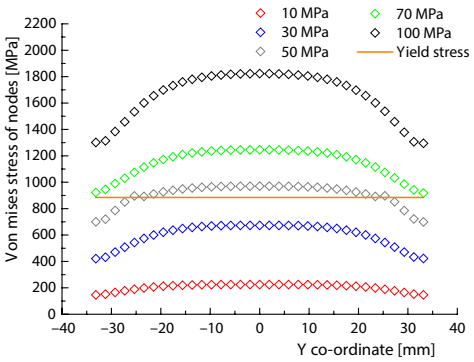

Figure 6. Nodes on the square cover Von Mises stress contours

Illustrated by the Von Mises stress contours in fig. 4, varying degrees of stress concentration which exceed the yield strength appears at the edge of square cover, E region in fig. 4(d). Pressure maintaining capacity is not insufficient. With the pressure increasing, the stress in D region at the center of the lower surface of the square cover, fig. 4(d), gradually increases to form a stress concentration area. In order to study this phenomenon, nodes on the lower surface in axial direction were taken as stress monitoring point, as shown by the dotted line in fig. 4(d). The nodal stress results under various conditions are shown in tab. 3 and fig. 6.

Table 3. Von Mises stress of nodes

Contents	Von Mises stress of nodes [MPa]				
	10 MPa	30 Mpa	50 MPa	70 MPa	100 MPa
Minimum value	146.88	422.66	699.45	918.48	1295.3
Maximum value	225.03	673.31	970.28	1246	1823.2
Difference	78.15	250.65	270.83	327.52	527.90

From the nodal stress calculation results in tab. 3 and fig. 4, maximum stress appears at the D region on the lower surface of the square cover, and the minimum stress appears at the C, F region on square cover. When pressure is 50 MPa, some nodal stress values exceed yield strength and enter in yield stage. Meanwhile, as the pressure increases, the stress concentration in the D region of the square cover enhances. It can be seen from fig. 6 that when the pressure is greater than 50 MPa, partial regions of the square cover begin to enter the yield stage, and as the pressure increases, the yield area of the square cover gradually increase. Indicating that present structure needs improvement to meet the requirements of deep coring.

Figure 7 shows the Von Mises stress contours of the base at several different pressure, the maximum stress of the base appears on the contact surface, as shown in G region in fig. 7(a). The value of maximum stress increases as the pressure increases. When the pressure is less than 70 MPa, the maximum stress of the base is less than the yield stress. and when the pressure is 100 MPa, the base begins to fail. Hence, base is harder to fail rather than the square cover under the same pressure condition.

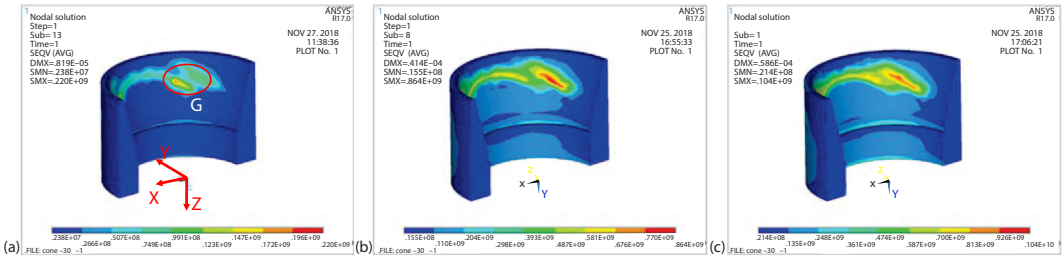

Figure 7. Von Mises stress contours of the base; (a) Von Mises stress contours (10 MPa), (b) Von Mises stress contours (70 MPa), and (c) Von Mises stress contours (100 MPa)
(*for color image see journal web site*)

In conclusion, the base is more reliable than square cover from the perspective of stress.

Optimal analysis of pressure controller

Pressure maintaining capacity of pressure controller is unsatisfied at present, especially for the square cover, which needs to be improved urgently. However, due to the particularity of the structure, the thickness of the square cover cannot be optimized. It can only be optimized from the following two aspects: the geometrical structure of the contact surface and the material property.

Optimization of contact surface structure

Pressure controller with conical sealing contact surface

Contact surface of present pressure controller is conical surfaces with an apex angle of 30°. Changing apex angle may have a great impact on the structure, so we changed apex angle to 25°, 35°, 40°, and 45°.

The maximum stress of the square cover of each scheme exceeded the yield strength under the pressure of 50 MPa. Therefore, only the calculation results of the cover under the pressure of 30 MPa are listed here. As shown in fig. 8, in some cases, the axial displacement distribution of the cover is consistent with the present pressure controller. Meanwhile, stress concentration likewise appears at the E region, shown in fig. 8(d). When the apex angle is 25°, the stress concentration reaches 904 MPa, which exceeds the yield stress, so this scheme is discarded.

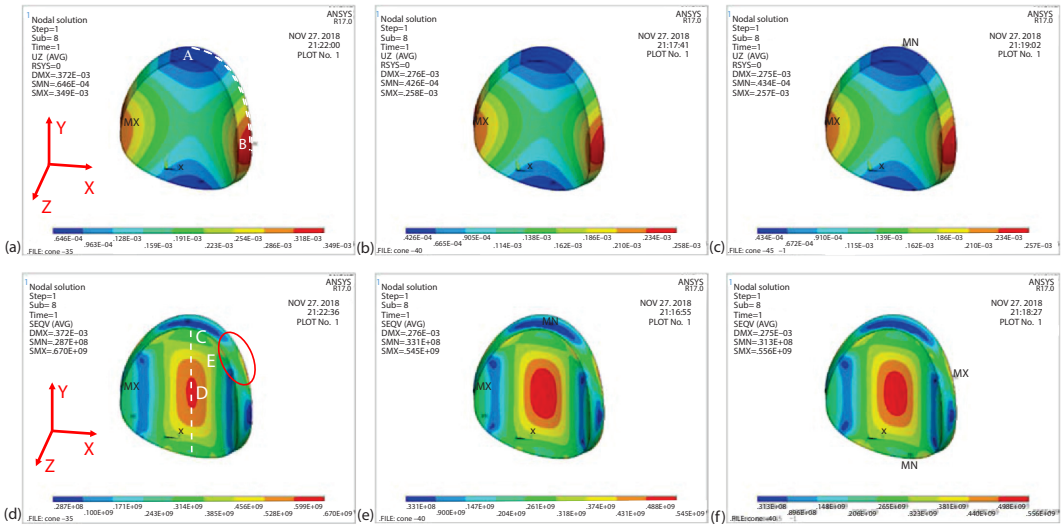

Figure 8. Axial displacement and Von Mises stress contours of contact surface of square cover with different apex angle (30 MPa); (a) axial displacement contours (35°), (b) axial displacement contours (40°), (c) axial displacement contours (45°), (d) Von Mises stress contours (35°), (e) Von Mises stress contours (40°), and (f) Von Mises stress contours (45°) (*for color image see journal web site*)

Node on the surface of the square cover was used as the displacement monitoring point, dotted line AB in fig. 8(a), and node on the axis of the lower surface of the square cover was used as the displacement monitoring point as well, dotted line in fig. 8(d). The calculation results of 30 MPa pressure are shown in tab. 4. After comparison, it is found that optimization scheme with 40° is optimal, and the pressure maintaining capacity of the square cover rise to 30 MPa.

Table 4. Comparison of optimization schemes for contact surface with different apex angle

Contents	Different angle [°]			
	30	35	40	45
Maximum displacement of square cover [mm]	0.45	0.35	0.26	0.26
Displacement difference of square cover [mm]	0.35	0.28	0.21	0.21
Maximum stress of square cover [MPa]	601	611.90	545	556
Base [MPa]	376	301	313	324

When pressure is 70 MPa, the maximum stress of base is 775 MPa, which is less than the yield stress. The stress is as high as 1040 MPa when 100 MPa is applied on, indicating that the base can withstand pressure of about 70 MPa.

It can be concluded that the 40° conical contact pressure controller has a pressure maintaining capacity of about 30 MPa (based on the square cover pressure maintaining capacity).

Pressure controller with spherical contact surface

It is critical to ensure that the pressure maintaining capacity of square cover may not fall due to position or angular offset. Besides, the contact area of the base was enlarged to

reduce stress concentration. We improved the conical contact surface to a spherical contact surface. The diameter of the bottom surface of the cone was taken as the diameter of the spherical.

Taking the results of 30 MPa and 50 Mpa as an example. As shown in the axial displacement contours in fig. 9, the minimum and maximum displacement still occur in the A and B regions, respectively. They are all smaller than the displacement of the square cover with 40° conical contact surface under the same pressure. Meanwhile, the displacement difference of the maximum and minimum displacement under the two pressure conditions is 0.19 mm, 0.31 mm, which is less than the value of 40° conical contact surface. As shown in fig. 9, the stress concentration in the E region almost completely disappears. On the contrary, there is still stress concentration in the D region of the square cover. When the pressure is 30 MPa, the maximum stress is 566.9 MPa, which is close to the value of 40° conical contact surface. The maximum stress exceeds the yield stress when the pressure is 50 MPa. Therefore,, the pressure maintaining capacity of square cover with spherical contact surface is about 30 MPa.

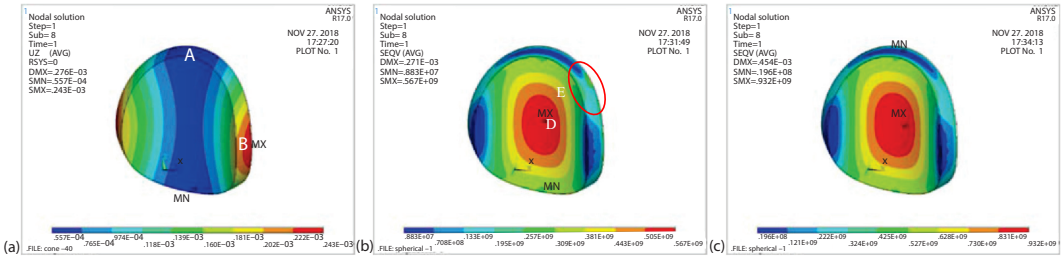

Figure 9. Axial displacement and Von Mises stress contours of square cover of pressure controller with spherical contact surface; (a) axial displacement contours (30 MPa), (b) Von Mises stress contours (30 MPa), and (c) Von Mises stress contours (50 MPa) (*for color image see journal web site*)

When the pressure is 100 MPa, the maximum stress of base still distributes on the contact face with the square cover. The maximum stress is 644 MPa, less than the yield stress, and is better than the 40° conical contact face.

In summary, pressure controller with the spherical contact surface is optimal in aforementioned structural optimization schemes. And the pressure maintaining capacity is about 30 MPa.

Material property optimization

Structural optimization can only improve its pressure maintaining capacity partially. It is necessary to choose better materials to meet the requirements of deep coring. The 45CrNiMoVA alloy is taken as an example, and the parameters are shown in tab. 5.

Table 5. Parameters of 45CrNiMoVA alloy

Materials	Elastic modulus [Pa]	Poisson ratio	Density[kgm^{-3}]	Yield stress [Pa]	Shear modulus [Pa]
45CrNiMoVA	2.14e11	0.29	7.83e3	1.33e9	8.28e10

After the material is optimized, the calculation results of square cover with spherical contact surface are shown in tab. 6. Obviously, the deformation and stress of the square cover have dropped. When the pressure reaches at 70 MPa, the maximum stress is 1327.7 MPa, which is close to the yield stress, indicating that the pressure maintaining capacity of the square cover is close to 70 MPa.

Table 6. Results of square cover of pressure controller with spherical contact surface after material optimization

Pressure	The maximum displacement [mm]	Displacement difference [mm]	The maximum Von Mises stress [MPa]
50 MPa	0.38	0.30	945.35
70 MPa	0.54	0.43	1327.7

When the pressure is 100 MPa, the maximum stress of base is 610 MPa, which is much smaller than the yield stress, indicating that the base pressure maintaining capacity is greater than 100 MPa.

After material optimization, pressure maintaining capacity of pressure controller with spherical contact surface increased to nearly 70 MPa.

Conclusions

The pressure controller is the indispensable component of the in-situ fidelity coring system. Based on the self-designed pressure controller, the pressure maintaining capacity is analyzed and optimized by numerical simulation.

- The square cover produces large deformation and significant stress concentration on the surface when self-designed pressure controller bears the pressure, which exceeds the yield stress. In such circumstances, the pressure controller has low pressure maintaining capacity.
- When the apex angle of the conical contact surface of the pressure controller improved to 25°, 35°, 40°, and 45°, the situation of deformation and stress concentration was improved. 40° of apex angle reinforced the pressure maintaining capacity to about 30 MPa.
- The contact surface was modified to a spherical surface, value of deformation largely reduced, and the stress concentration at the edge of the square cover disappeared. Pressure maintaining capacity was around 30 MPa.
- The material was improved to 45CrNiMoVA alloy, and the pressure maintaining capacity of the spherical contact surface pressure controller rose to nearly 70 MPa, indicating that the pressure controller after optimization is suitable for deep earth where osmotic pressure is nearly 70 MPa.

Acknowledgment

This work was financially supported by the State Key Research Development Program of China (Grant No. 2016YFC0600701), National Natural Science Foundation of China (Grant No. 51822403,Grant No. 51674170).

References

[1] Xie, H. P., *et al.*, Research and Development of Rock Mechanics in Deep Ground Engineering, *Chinese Journal of Rock Mechanics and Engineering*, *34* (2015), 11, pp. 2161-2178
[2] Xie, H. P., *et al.*, Quantitative Definition and Investigation of Deep Mining, *Journal of China Coal Society*, *40* (2015), 1, pp. 1-10
[3] Xie, H. P., Research Framework and Anticipated Results of Deep Rock Mechanics and Mining Theory, *Advanced Engineering Sciences*, *49* (2017), 2, pp. 1-16
[4] Gao, M., *et al.*, Field Experiments on Fracture Evolution and Correlations Between Connectivity and Abutment Pressure under Top Coal Caving Conditions, *International Journal of Rock Mechanics and Mining Science*, *111* (2018), Oct., pp. 84-93
[5] Coney, L., *et al.*, Geochemistry of Impactites and Basement Lithologies from ICDP Borehole LB - 07A, Bosumtwi Impact Structure, Ghana, *Meteoritics and Planetary Science, 42* (2007), 4-5, pp. 667-688

[6] Dickens, G. R., *et al.*, The Pressure Core Sampler (PCS) on ODP Leg 201: General Operations and Gas Release, *Proceedings*, The Ocean Drilling Program, Texas A and M University, Texas, US, 2003, Vol. 201
[7] Litt, T., *et al.*, PALEOVAN, International Continental Scientific Drilling Program (ICDP): Site Survey Results and Perspectives, *Quaternary Science Reviews*, *28* (2009), 15, pp. 1555-1567
[8] Yun, T. S., Mechanical and Thermal Study of Hydrate Bearing Sediments, Ph. D. thesis, Georgia Institute of Technology, Atlanta, Geo., USA, 2005
[9] Fridleifsson, G. O., *et al.*, The Iceland Deep Drilling Project 4.5 Km Deep Well, IDDP-2, inthe Sea-water-Recharged Reykjanes Geothermal Field inSW IcelandHas Successfully Reached Its Supercritical Target, *Scientific Drilling*, *23* (2017), 5, pp.1-12
[10] Yun, T. S., *et al.,* Hydrate-Bearing Sediments from the Krishna − Godavari Basin: Physical Characterization, Pressure Core Testing, and Scaled Production Monitoring, *Energy and Fuels*, *24* (2010), 11, pp. 5972-5983
[11] Wang, W. S., *et al.*, Key Technology of Coring in Hard Rocks for Scientific Ultra-Deep Drilling, *Exploration Engineering (Rock and Soil Drilling and Tunneling)*, *41* (2014), 1, pp. 9-12
[12] Rothwell, R. G., Rack, F. R.,New Techniques in Sediment Core Analysis: an Introduction, *Geological Society, London, Special Publications*, *267* (2006), 1, pp. 1-29
[13] Schultheiss, P., *et al.*, Wireline Coring and Analysis under Pressure: Recent Use and Future Developments ofthe HYACINTH System, *Scientific Drilling*, *7* (2009), Mar, pp. 44-50
[14] Wakishima, R., The Development ofaPressure Temperature Core Sampler (PTCS) forthe Recovery of-In-Situ Methane Hydrates, *Proceedings*, The International Symposium on Methane Hydrates, JNOC-TRC, Tokyo, Japan, 1998, Vol. 107
[15] Bohrmann G., *et al.*, Appearance and Preservation of Natural Gas Hydrate From Hydrate Ridge Sampled During ODP Leg 204 Drilling, *Marine Geology*, 244 (2007), 1, pp. 1-14
[16] Hohnberg H. J.,*et al.*, Pressurized Coring of Near-Surface Gas-Hydrate Sediments on Hydrate Ridge: The Multiple Autoclave Corer and First Results from Pressure-Core X-Ray CT Scans, *Proceedings*, EGS-AGU-EUG Joint Assembly, Nice, France, 2003, Vol. 5
[17] Qin, H. W., *et al.*, Pressure Tight Piston Corer – A New Approach on Gas Hydrate Investigation, *China Ocean Engineering*, *19* (2005), 1, pp. 121-128
[18] Chen, Y., *et al.*, Research on Pressure Tight Sampling Technique of Deep-Sea Shallow Sediment – A New Approach to Gas Hydrate Investigation, *China Ocean Engineering*, *20* (2006), 4, pp. 657-664
[19] Li, S. L., *et al.*, Development of Pressure Piston Corer for Exploring Natural Gas Hydrates, *Journal of Zhejiang University (Engineering Science)*, *40* (2006), 5, pp. 888-892

Paper submitted: June 12, 2018
Paper revised: July 11, 2018
Paper accepted: December 18, 2018